

No Internal/External Offsets in the FOS/BLUE Wavelength Calibration

F. Kerber, A. Alexov, P. Bristow, V. Luridiana & M. R. Rosa

December 2001

Abstract

FOS/BLUE observations of the dM1e star AU Mic have been used to look for systematic offsets between the wavelength scales obtained from an external source and the internal calibration lamp. Contrary to earlier reports, we do not see any systematic offsets when using data from the POA corrected archive. We conclude that the previously reported offsets had been introduced by the deficiencies of the original calibration.

1. Introduction

Systematic offsets between wavelengths derived from the internal calibration (PtCr-Ne hollow cathode) lamps and external sources have been reported for the **Faint Object Spectrograph (FOS)**, both pre-launch and on orbit (Sirk & Bohlin, 1987; Bohlin, Sirk, Hartig, 1987; Blair, Kriss, Davidsen 1988, Kriss, Blair, Davidsen 1992).

Observations dedicated to this investigation were done in September 1991 during science verification (proposal 3316). On the blue side, exposures using gratings G130H, G190H and G160L of the M1Ve star AU Mic (HD 197481, $\alpha = 20\ 45\ 09.53$ $\delta = -31\ 20\ 27.2$, 2000.0) were obtained.

This star is a very interesting object scientifically, see e.g. Pagano et al., (2000). In this context it is only important to mention that it has a typical late-type star spectrum with additional Balmer series emission lines and a very low heliocentric radial velocity. The most reliable ground based measurements seem to be from the work of Bopp & Fekel (1977), who derived its velocity to be -2.1 ± 1.0 km/s. When using only the (~ six) emission lines, the velocity error was even smaller, at -2.1 ± 0.6 km/s. Other values quoted in literature range from -4 to $+5$ km/s. Observations using the **Goddard High Resolution Spectrograph (GHRS)** (Linsky & Wood 1994) gave a radial velocity of 1.0 ± 1.6 km/s from the Si IV (1393 Å, 1402 Å) and C IV (1548 Å, 1550 Å) doublets in emission. The more recent **Space Telescope Imaging Spectrograph (STIS)** observations using the medium resolution echelle grating E140M cover the range 1170 to 1710 Å. They find a photospheric radial velocity of -5.7 ± 0.3 km/s from 37 C I lines. The emission lines are found to be redshifted by about 2 km/s with respect to this value (Pagano et al., 2000). Additional details of the FOS observations can be found in ISR 70 (Kriss, Blair, Davidsen 1992).

2. Data

We have looked at the available FOS/BLUE observations of AU Mic taken in 1991 (datasets y0q7*). Out of those, we used the data from the two high resolution gratings G130H and G190H (Table 2). All the files are taken from the POA corrected FOS archive provided by the ST-ECF <http://www.stecf.org/poa/pcrel/archdata.html> and <http://archive.eso.org/wdb/wdb/hst/science/form>. See ISR POA/FOS-2001-8 for details of the recalibration work.

As has been previously reported (STScI CAL/FOS ISR #70), all exposures are underexposed, especially in the H13 grating, therefore a careful analysis is required for this purpose. The emission lines were measured interactively in the pixel domain (.c4 files) using the IRAF *splot*

task. The values were then converted to wavelengths using the new *STPOA pix2wav* tool, which is an implementation of the dispersion solution derived from the internal calibration lamp (POA_FOS-2001-xx). Additionally, we used the IRAF task *mkmultispec* to combine the .c0 (wavelength info) and .c1 (counts information in pixel space) files to form a wavelength calibrated spectrum for comparison. The results were practically identical.

While individual users may choose to use different tools or methods, this sequence of steps is a standard way of performing data reduction and analysis. The measured wavelengths were corrected for barycentric motion but not for the orbital motion of the HST.

3. Results

Due to the weak exposures, the number of usable lines is limited. Four exposures were available in both the G130H and G190H gratings and all were analyzed in detail, see Table 2 in the appendix. Note that two digits are used throughout in order to minimize round off errors; this does not imply that the velocities can be measured to this accuracy.

The results are internally fully consistent for all the observations but due to the marginally usable S/N ratio of the shorter exposures the errors on the velocity values are very large (50 to 100 km/s). We therefore selected the longest exposures (G130H: y0q701ht; G190H: y0q7010et) for more detailed presentation.

The Lyman α emission line is not usable because of the coincident Geocoronal emission and because of its complex shape, see Fig. 23 in Heap et al. (1995). Note that this line had been used in previous analyses.

After careful examination, a total of 16 usable lines could be extracted, resulting in an average radial velocity of -3.2 ± 17.6 km/s. Note that the values derived for G130H and G190H separately, are fully consistent at -1.4 ± 27.2 km/s (six lines) and -4.2 ± 9.3 km/s (ten lines).

The above resultant value is in excellent agreement with the literature value of -2.1 ± 1.0 km/s. Another meaningful comparison is with the STIS observations of the same lines (Pagano et al, 2000). From the five emission lines in common, we get an average radial velocity of -3.4 ± 2.6 km/s. See Table 1 for the individual velocities and Fig. 1 for a graphical presentation.

• **Table 1:** Radial velocities of the emission lines in the best S/N FOS exposures of AU Mic. Recent STIS measurements (Pagano et al., 2000) are given for comparison.

Ion	λ_0 [Å]	λ_{obs} [Å]	v_{obs} [km/s]	$v_{\text{corrected}}$ [km/s]	v_{helio} [km/s]
Y0Q701HT					STIS
Lyman α	1215.668	1214.641	-253.25	-283.06	
Lyman α	1215.668	1216.260	146.23	116.41	
O I	1304.858	1305.737	202.10	172.95	
O I	1305.708	1305.737	6.69	-22.44	-6.4
C II	1334.531	1334.497	-7.69	-36.64	0.5
C II	1335.708	1335.819	24.96	-3.97	-3.6
C IV	1548.184	1548.494	60.08	32.33	-2.7
C IV	1550.773	1550.889	22.28	-5.47	-4.6
C I	1561.120	1561.409	55.54	27.83	
6 lines				-1.39 \pm 27.20	-3.36 \pm 2.56
Y0Q701ET					
He II	1640.458	1640.643	33.760	-17.69	
C I	1657.196	1657.513	57.471	6.31	
Si II	1808.012	1808.324	51.749	3.19	
Si II	1816.928	1817.210	46.527	-1.92	
Al III	1854.716	1854.993	44.775	-3.10	
C I	1930.905	1931.182	42.987	-3.78	
C I	1993.620	1993.889	40.412	-5.50	
Fe II	2260.781	2261.012	30.649	-12.22	
Fe II	2261.560	2261.971	54.502	11.63	
Fe II	2280.620	2280.800	23.603	-19.05	
10 lines				-4.21 \pm 9.28	
Y0Q701HT & Y0Q701ET					STIS
16 lines				-3.16 \pm 17.55	-3.36 \pm 2.56

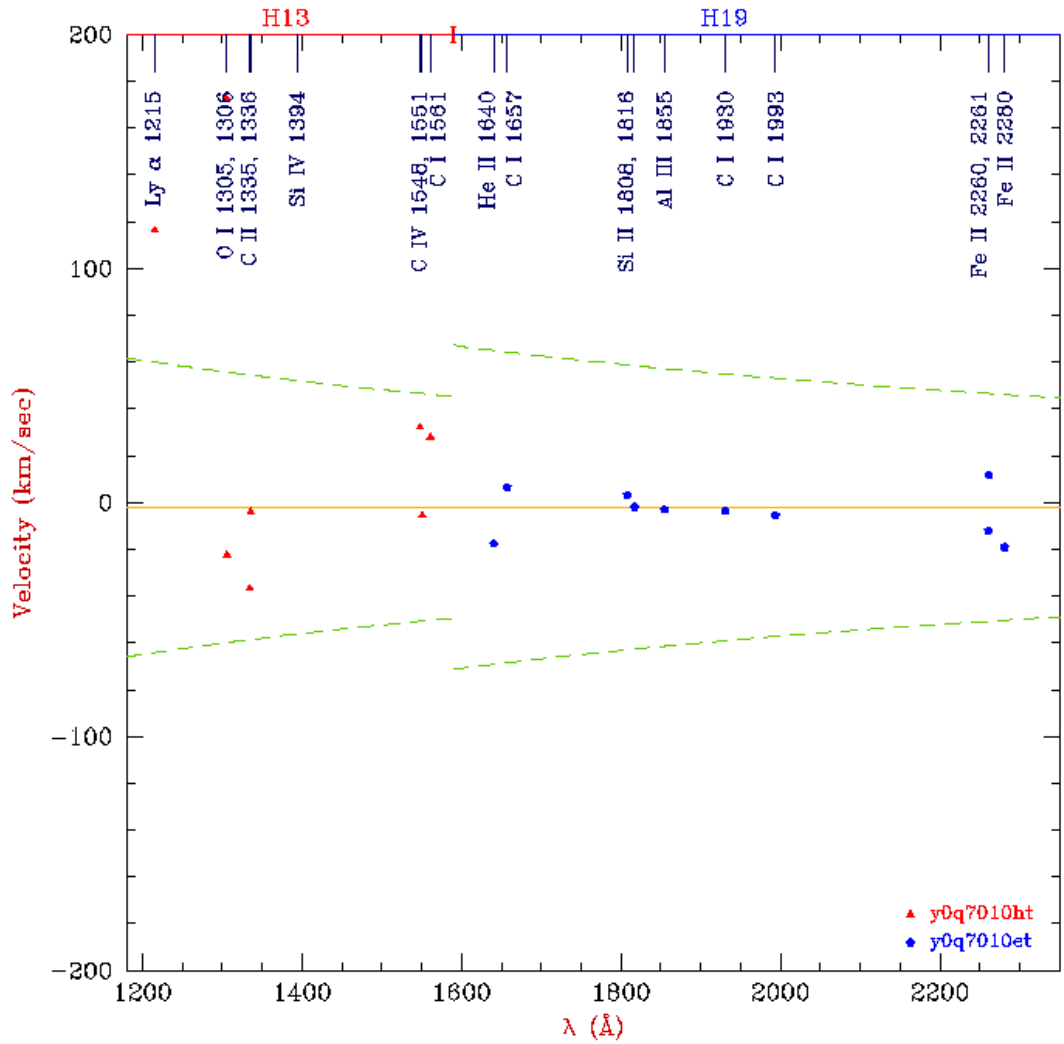


Figure 1: Heliocentric radial velocities of the emission lines in AU Mic measured on the two longest exposures. Note the larger scatter in the G130H data due to the lower S/N. The dashed lines indicate a shift in velocity of ± 1 pixel.

4. Discussion

Previous studies had reported systematic offsets between internal and external wavelength scales. The most recent published value had been -0.102 ± 0.100 diodes or -23.3 ± 22.8 km/s (Kriss et al., 1992). While this value does not represent a significant offset, the authors maintain that systematic offsets between internal and external wavelength scales have always been present pre-launch and on-orbit.

Using the POA corrected data we have not found any significant offset from the same raw data. We obtained an average radial velocity of -3.2 ± 17.6 km/s, which is indistinguishable from the literature value of -2.1 ± 1.0 km/s and is almost identical to the value of -3.4 ± 2.6 km/s found from STIS observations of five of the same lines.

The difference to the previously reported offset is equivalent to half a pixel shift in the zero-point of the wavelength solution. This value is very close to the net effect of the various POA corrections for the data and we therefore conclude that the previously reported offsets were the result of the deficiency of the original pipeline calibration and the GIMP correction.

We therefore conclude that there was never an offset between internal and external wavelength scales on the BLUE side of the FOS.

5. References

Blair, W.P., Kriss, G.A., Davidsen, A.F., 1988, CAL/FOS-056, FOS Internal/External Offsets

Bohlin, R., Sirk, M., Hartig G., 1987, CAL/FOS-044, Limiting Accuracy of the FOS Wavelength Calibration

Bopp, B.W., Fekel, Jr., F., 1977, AJ 82, 490

Heap, S.R., Brandt, J.C., Randall, C.E. et al., 1995, PASP 107, 871

Junkarrinen, V., Beaver, E., Cohen, R., Lyons, R., 1990, CAL/FOS-066, Sensitivity of the FOS Red Digicon to External B-fields

Kriss, G.A., Blair, W.P., Davidsen, A.F., 1988, CAL/FOS-054, Revised FOS Wavelength Calibration

Kriss, G.A., Blair, W.P., Davidsen, A.F., 1992, CAL/FOS-070, Internal/External Offsets in the FOS Wavelength Calibration

Linsky, J.L., Wood, B.E., 1994, ApJ 430, 342

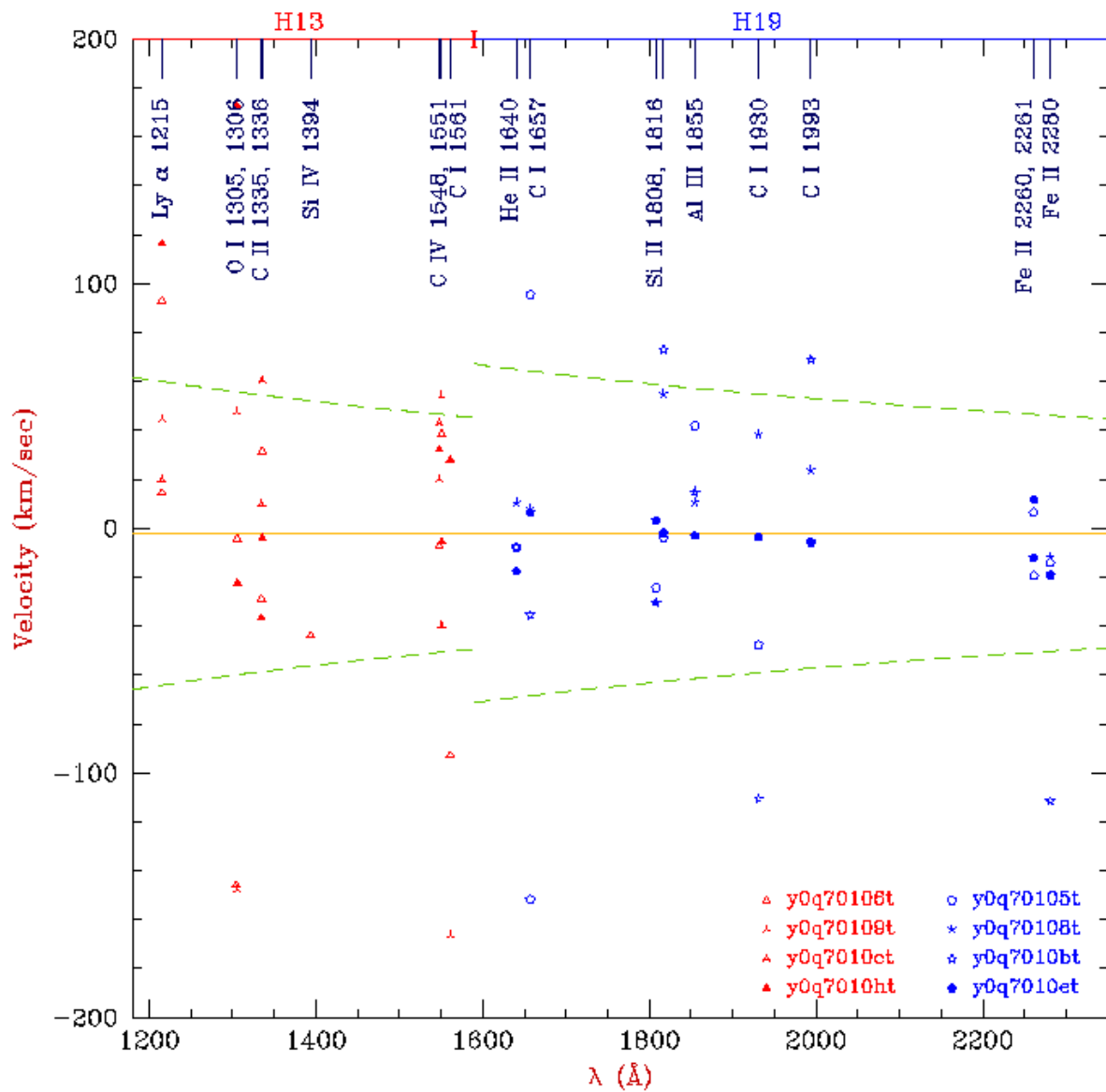
Pagano, I., Linsky, J.L., Carkner, L., Robinson, R.D., Timothy, G., 2000, ApJ 532, 497

Sirk, M., Bohlin, R., 1987, CAL/FOS-041, Wavelength Offsets among the Internal Lamps and External Sources

Appendix

• **Table 2:** Basic data of all FOS/BLUE side observations of AU Mic

Root Name	Start (Date Time [UT])	T_exp [s]	Filter	Aperture
Y0Q70101T	10 Sep 1991 19:31:24	1.200	G400H	
Y0Q70102T	10 Sep 1991 20:53:13	12.000	G400H	
Y0Q70103T	10 Sep 1991 21:06:18	25.000	G400H	
Y0Q70104T	10 Sep 1991 22:17:27	25.000	G400H	
Y0Q70105T	10 Sep 1991 22:39:29	116.999	G190H	B-1
Y0Q70106T	10 Sep 1991 22:45:18	52.000	G130H	B-1
Y0Q70107T	10 Sep 1991 22:49:32	52.000	G160L	B-1
Y0Q70108T	10 Sep 1991 22:55:17	81.000	G190H	B-3
Y0Q70109T	10 Sep 1991 23:00:24	36.000	G130H	B-3
Y0Q7010AT	10 Sep 1991 23:53:07	36.000	G160L	B-3
Y0Q7010BT	10 Sep 1991 23:59:34	45.000	G190H	A-1
Y0Q7010CT	10 Sep 1991 00:04:01	20.000	G130H	A-1
Y0Q7010DT	10 Sep 1991 00:07:59	20.000	G160L	A-1
Y0Q7010ET	10 Sep 1991 00:14:36	160.000	G190H	B-2
Y0Q7010HT	10 Sep 1991 00:27:52	70.000	G130H	B-2
Y0Q7010IT	10 Sep 1991 00:32:41	70.000	G160L	B-2
Y0Q7010LT	10 Sep 1991 01:44:36	116.999	G190H	C-2
Y0Q7010MT	10 Sep 1991 01:50:23	52.000	G130H	C-2
Y0Q7010NT	10 Sep 1991 01:54:39	52.000	G160L	C-2
Y0Q7010KT	10 Sep 1991 01:36:00	7.000	MIRROR	



• **Figure 2:** Heliocentric radial velocities of the emission lines in AU Mic measured on all available G130H and G190H exposures. Note the larger scatter due to the limited S/N of most exposures. The dashed lines indicate a shift in velocity of ± 1 pixel.

• **Table 3:** Radial velocities of the emission lines in the G130H exposures of AU Mic.

Ion	λ_0 [Å]	λ_{obs} [Å]	v_{obs} [km/s]	v_{subpix} [km/s]	v_{bary} [km/s]	$v_{corrected}$ [km/s]
Y0Q70106T						
Lyman α	1215.668	1215.827	39.30	-4.962	-19.93	14.40
Lyman α	1215.668	1216.146	117.98	-4.963	-19.93	93.08
O I	1304.858	1304.330	-121.36	-4.624	-19.93	-145.92
O I	1305.708	1305.796	20.31	-4.621	-19.93	-4.26
C II	1334.531	1334.512	-4.31	-4.521	-19.93	-28.76
C II	1335.708	1335.957	55.93	-4.517	-19.93	31.46
Si IV	1393.755	1393.664	-19.47	-4.329	-19.93	-43.73
C IV	1548.184	1548.269	16.38	-3.897	-19.93	-7.45
C IV	1550.773	1551.095	62.16	-3.890	-19.93	38.33
C I	1561.120	1560.761	-69.02	-3.865	-19.93	-92.81
3 lines					-17.17 \pm 49.20	
Y0Q70109T						
Lyman α	1215.668	1215.955	71.92	-7.382	-19.96	44.60
O I	1304.858	1305.181	74.39	-6.879	-19.96	47.53
O I	1305.708	1305.181	-120.93	-6.873	-19.96	-147.77
C IV	1548.184	1548.420	45.63	-5.797	-19.96	19.88
C IV	1550.773	1551.185	79.72	-5.787	-19.96	53.97
C I	1561.120	1560.387	-140.89	-5.749	-19.96	-166.60
3 lines					-30.92 \pm 118.74	
Y0Q7010CT						
Lyman α	1215.668	1215.863	48.28	-8.375	-20.07	19.85
C II	1334.531	1334.699	37.55	-7.629	-20.07	9.88
C II	1335.708	1336.101	88.30	-7.622	-20.07	60.62
C IV	1548.184	1548.545	69.84	-6.576	-20.07	43.20
C IV	1550.773	1550.705	-13.30	-6.565	-20.07	-39.93
4 lines					18.44 \pm 44.24	
Y0Q7010HT						
Lyman α	1215.668	1214.641	-253.25	-9.616	-20.20	-283.06
Lyman α	1215.668	1216.260	146.23	-9.616	-20.20	116.41
O I	1304.858	1305.737	202.10	-8.958	-20.20	172.95
O I	1305.708	1305.737	6.69	-8.953	-20.20	-22.44
C II	1334.531	1334.497	-7.69	-8.759	-20.20	-36.64
C II	1335.708	1335.819	24.96	-8.752	-20.20	-3.97
C IV	1548.184	1548.494	60.08	-7.551	-20.20	32.33
C IV	1550.773	1550.889	22.28	-7.538	-20.20	-5.47
C I	1561.120	1561.409	55.54	-7.488	-20.20	27.83
6 lines					-1.39 \pm 27.20	

• **Table 4:** Radial velocities of the emission lines in the G190H exposures of AU Mic.

Ion	λ_0 [Å]	λ_{obs} [Å]	v_{obs} [km/s]	v_{subpix} [km/s]	v_{bary} [km/s]	$v_{\text{corrected}}$ [km/s]
Y0Q70105T						
He II	1640.458	1640.639	33.044	-21.20	-19.92	-8.05
C I	1657.195	1656.583	-110.918	-20.98	-19.92	-151.80
C I	1657.195	1657.949	136.399	-20.98	-19.92	95.52
Si II	1808.011	1808.102	14.985	-19.23	-19.92	-24.16
Si II	1816.928	1817.141	35.190	-19.14	-19.92	-3.86
Al III	1854.715	1855.215	80.681	-18.75	-19.92	42.06
C I	1930.905	1930.842	-9.781	-18.01	-19.92	-47.71
C I	1993.619	1993.830	31.686	-17.44	-19.92	-5.69
Fe II	2260.781	2261.095	41.699	-15.38	-19.92	6.40
Fe II	2261.560	2261.680	15.879	-15.37	-19.92	-19.42
Fe II	2280.620	2280.781	21.100	-15.25	-19.92	-14.09
9 lines					-8.28 ± 24.34	
Y0Q70108T						
He II	1640.458	1640.760	55.218	-24.95	-19.95	10.31
C I	1657.196	1657.485	52.357	-24.70	-19.95	7.70
Si II	1808.011	1808.087	12.410	-22.64	-19.95	-30.19
Si II	1816.928	1817.518	97.346	-22.53	-19.95	54.87
Al III	1854.716	1855.041	52.571	-22.07	-19.95	10.56
C I	1930.905	1931.416	79.429	-21.20	-19.95	38.27
C I	1993.620	1994.047	64.230	-20.53	-19.95	23.72
Fe II	2280.620	2280.820	26.286	-17.95	-19.95	-11.62
8 lines					12.95 ± 28.90	
Y0Q7010BT						
He II	1640.458	1640.681	40.734	-28.30	-20.06	-7.65
C I	1657.196	1657.266	12.589	-28.02	-20.06	-35.49
Si II	1808.012	1808.104	15.271	-25.68	-20.06	-30.47
Si II	1816.928	1817.647	118.661	-25.56	-20.06	73.07
Al III	1854.716	1855.086	59.903	-25.03	-20.06	14.77
C I	1930.905	1930.477	-66.519	-24.05	-20.06	-110.63
C I	1993.620	1994.366	112.259	-23.29	-20.06	68.92
Fe II	2280.620	2280.080	-71.043	-20.36	-20.06	-111.45
8 lines					-17.32 ± 76.12	
Y0Q7010ET						
He II	1640.458	1640.643	33.760	-31.39	-20.09	-17.69
C I	1657.196	1657.513	57.471	-31.07	-20.09	6.31
Si II	1808.012	1808.324	51.749	-28.48	-20.09	3.19
Si II	1816.928	1817.210	46.527	-28.34	-20.09	-1.92
Al III	1854.716	1854.993	44.775	-27.76	-20.09	-3.10
C I	1930.905	1931.182	42.987	-26.67	-20.09	-3.78
C I	1993.620	1993.889	40.412	-25.83	-20.09	-5.50
Fe II	2260.781	2261.012	30.649	-22.78	-20.09	-12.22
Fe II	2261.560	2261.971	54.502	-22.77	-20.09	11.63
Fe II	2280.620	2280.800	23.603	-22.58	-20.09	-19.05
10 lines					-4.21 ± 9.28	